

Investigation on energy dissipation and its mechanism of coal under dynamic loads

Junjun Feng^{1,2}, Enyuan Wang^{*1,2}, Rongxi Shen^{1,2},
Liang Chen^{1,2}, Xuelong Li^{1,2} and Zhaoyong Xu^{1,2}

¹ Key Laboratory of Gas and Fire Control for Coal Mines,
China University of Mining and Technology, Xuzhou, 221116, China

² Faculty of Safety Engineering, China University of Mining and Technology, Xuzhou, 221116, China

(Received December 02, 2015, Revised May 20, 2016, Accepted June 10, 2016)

Abstract. The energy dissipation of coal under dynamic loads is a major issue in geomechanics and arising extensive concerns recently. In this study, dynamic loading tests of coal were conducted using a split Hopkinson pressure bar (SHPB) system, the characteristics of dynamic behavior and energy dissipation of coal were analyzed, and the mechanism of energy dissipation was discussed based on the fracture processes of coal under dynamic loads. Experimental results indicate that the energy dissipation of coal under dynamic loads has a positive linear correlation with both incident energy and dynamic compressive strength, and the correlation coefficients between incident energy, dynamic compressive strength and the energy dissipation rate are 0.74 and 0.98, respectively. Theoretical analysis demonstrates that higher level of stress leads to greater energy released during unstable crack propagation, thus resulting in larger energy dissipation rate of coal under dynamic loads. At last, a semi-empirical energy dissipation model is proposed for describing the positive relationship between dissipated energy and stress.

Keywords: split Hopkinson pressure bar; energy dissipation; incident energy; dynamic compressive strength; fracture processes

1. Introduction

Dynamic behavior of coal and rock is one of the most significant issues encountered in various underground engineering, such as coal mining, tunnel excavation, civil construction, and blasting (Yang *et al.* 2014, Zhang and Zhao 2014). Considerable research effort has been devoted to characterize the dynamic behavior of coal and rock, and the results indicate that the failure process of brittle materials under dynamic loads is always linked to the energy dissipation (Gaziev 2001). Therefore, a thorough understanding on the energy dissipation features and its mechanism of coal and rock is theoretically and practically significant for dealing with the failure issues encountered in underground engineering.

Many tests have been conducted to investigate the energy dissipation of coal and rock under different loading conditions, including quasi-static loads and dynamic loads. Since the rock deformation and destruction under quasi-static loads was considered as an irreversible process of

*Corresponding author, Professor, E-mail: weycumt@126.com

energy dissipation (Xie *et al.* 2011), many scholars have studied the energy dissipation of rock under different quasi-static loading conditions, such as uniaxial compression (Song *et al.* 2015, Sufian and Russell 2013, Wasantha *et al.* 2014), conventional triaxial unloading (Huang and Li 2014). A few others have also studied the energy dissipation of coal under uniaxial cyclic loading (Song *et al.* 2012) and conventional triaxial loading conditions (Peng *et al.* 2015). These studies show that the energy dissipation of coal and rock under quasi-static loads is closely related to external loading conditions.

The research on energy dissipation of rock under dynamic loads was mainly conducted using split Hopkinson pressure bar (Zhang and Zhao 2014). The energy dissipation of rock under dynamic loads was first studied by Lundberg (Lundberg 1976) using an SHPB system. Numerous studies have suggested that the energy dissipation of rock under dynamic loads is related to strain rate (Liu *et al.* 2012), slenderness ratio (Li *et al.* 2014), incident energy (Hong *et al.* 2009), and fragmentation (Whittles *et al.* 2006). However, the underlying mechanism of energy dissipation of coal is still unclear, thus systematic and specialized investigations on the mechanism of energy dissipation of coal under dynamic loads is quite necessary, which could provide a theoretical basis for understanding the energy dissipation of coal. In this study, a series of dynamic loading tests were conducted using the SHPB system, and the characteristics of dynamic behavior and energy dissipation of coal are studied. Furthermore, the mechanism of energy dissipation is discussed from the perspective of dynamic fracture processes, and a semi-empirical energy dissipation model is finally proposed for describing the positive relationship between dissipated energy and stress. The results obtained in this paper provide a theoretical basis for dealing with the various failure issues encountered in underground engineering, such as coal mining, tunnel excavation, civil construction, and blasting engineering.

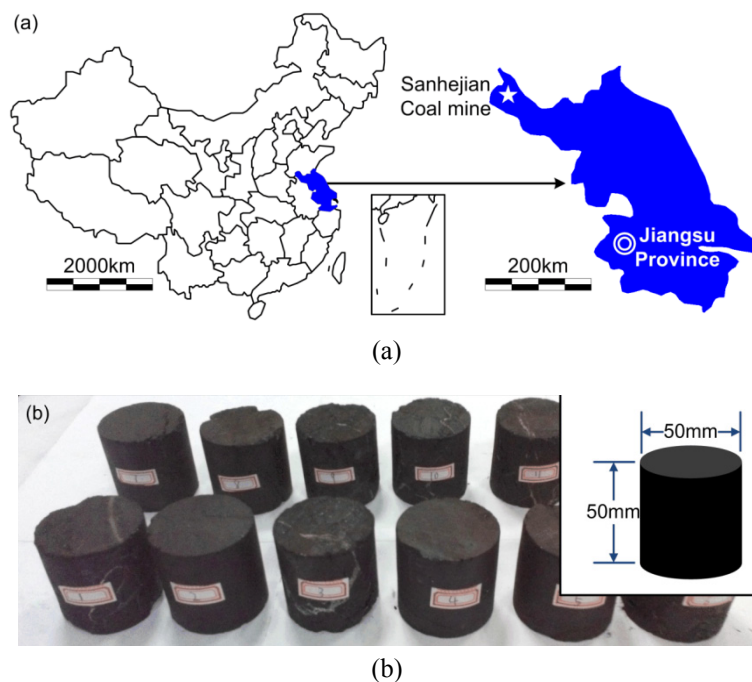


Fig. 1 Information of coal specimens

Table 1 Physical properties, thermal property, and proximate analysis result of Sanhejian coal specimens

| Physical properties | | Proximate analysis | | | Thermal property |
|-----------------------------------|---------------------------------------|--------------------|---------|---------------------|-------------------------|
| True density (kg/m ³) | Apparent density (kg/m ³) | Moisture (%) | Ash (%) | Volatile matter (%) | Calorific value (MJ/kg) |
| 1446 | 1541 | 2.1 | 26.27 | 37.53 | 23.15 |

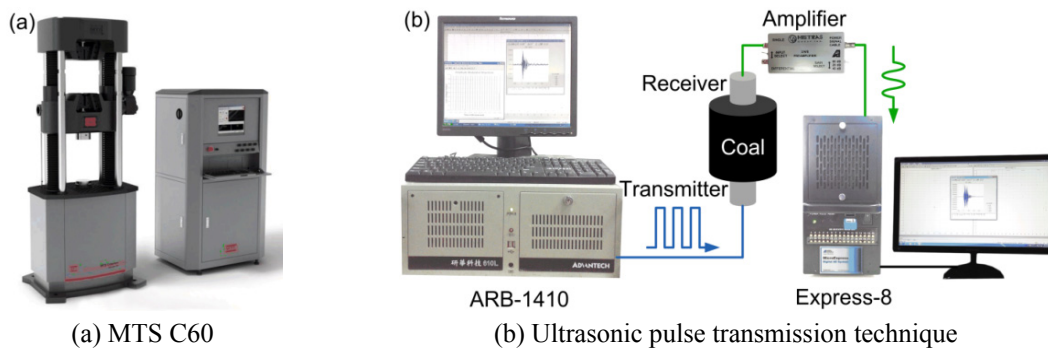


Fig. 2 Experimental system for determining quasi-static mechanical properties of coal specimens

Table 2 Quasi-static mechanical properties, wave velocities of Sanhejian coal specimens

| Mechanical properties | | | Wave velocities | |
|-------------------------------------|-----------------------|-----------------|-------------------------|------------------|
| Uniaxial compressive strength (MPa) | Young's modulus (GPa) | Poisson's ratio | Dilatational wave (m/s) | Shear wave (m/s) |
| 8.77 | 4.74 | 0.40 | 2126.89 | 1074.24 |

2. Methods

2.1 Specimen preparation and basic properties

Coal samples were obtained from the Sanhejian coal mine located in Jiangsu Province (Fig. 1(a)). In accordance with the recommended specimen size for SHPB experiments (Davies and Hunter 1963), the samples were processed uniformly through drilling from the raw coal blocks along parallel bedding directions, then slicing and polishing into cylindrical specimens (Fig. 1(b)-(c)). The roughness at both ends of the polished specimens is less than 0.02 mm, and the ends of these polished specimens are perpendicular to their axial line. The maximum angle of deviation between each end of polished specimen and the axial line of specimen is less than 0.25°. Physical properties, thermal property, and proximate analysis result of Sanhejian coal specimens are listed in Table 1 as an essential part of the basic description for specimens.

Quasi-static mechanical properties of Sanhejian coal are obtained using a MTS C60 hydraulic servo-control testing machine (Fig. 2(a)) based on the ISRM suggested method (Bieniawski and Bernede 1979). The results are listed in Table 2, including uniaxial compressive strength, Young's modulus, and Poisson's ratio. In addition, the wave velocities of Sanhejian coal are determined by

$$\dot{\varepsilon}(t) = \frac{C}{L_0} [\varepsilon_i(t) - \varepsilon_r(t) - \varepsilon_t(t)] \quad (1)$$

$$\varepsilon(t) = \frac{C}{L_0} \int_0^t [\varepsilon_i(t) - \varepsilon_r(t) - \varepsilon_t(t)] dt \quad (2)$$

$$\sigma(t) = \frac{AE}{2A_0} [\varepsilon_i(t) + \varepsilon_r(t) + \varepsilon_t(t)] \quad (3)$$

where $\dot{\varepsilon}(t)$ is the strain rate, $\varepsilon(t)$ is the strain, $\sigma(t)$ is the stress, C is the longitudinal wave velocity of bar, L_0 is the sample thickness, A is the cross-sectional area of bar, A_0 is the cross-sectional area of specimen, ε denotes strain, and the subscripts i , r , t refer to the incident, reflected and transmitted waves, respectively. The dissipated energy of coal specimen under dynamic loads can be calculated as follows (Lundberg 1976)

$$W_c = W_i - (W_r + W_t) \quad (4)$$

where W_c is the dissipated energy of coal specimen, W_i , W_r , and W_t are energy carried by the incident, reflected, and transmitted wave, respectively, which can be calculated as follows

$$W_i = A_e E c_e \int_0^\tau \varepsilon_i^2(t) dt \quad (5)$$

$$W_r = A_e E c_e \int_0^\tau \varepsilon_r^2(t) dt \quad (6)$$

$$W_t = A_e E c_e \int_0^\tau \varepsilon_t^2(t) dt \quad (7)$$

where τ is the duration of stress wave, $\rho_e c_e$ is the wave impedance of bars, A_e is the cross-sectional area of bars, $\sigma(t)$ denotes stress in bar at time t , and the subscripts i , r , t refer to the incident, reflected and transmitted waves, respectively. To eliminate the influence of the amplitude fluctuation of incident wave, the energy dissipation rate of specimen is defined as w_c , which is a dimensionless quantity, and its expression is as follows

$$w_c = W_c / W_i \quad (8)$$

3. Results

3.1 Characteristics of dynamic behavior

The experiments were conducted using the SHPB system shown in Fig. 3, and the results are listed in Table 3, which indicate that the range of impact velocity is 10.47–13.49 m/s; the range of strain rate of coal is 44.40–66.69 s⁻¹; and the range of dynamic compressive strength of coal is 5.41–18.70 MPa.

Table 3 Strain rate and dynamic compressive strength (σ_d) of coal under dynamic loads

| Sample ID | Diameter (mm) | Length (mm) | Impact velocity (m/s) | Strain rate (s^{-1}) | σ_d (MPa) |
|-----------|---------------|-------------|-----------------------|--------------------------|------------------|
| M1 | 49.80 | 49.90 | 13.28 | 62.70 | 18.70 |
| M2 | 48.50 | 49.80 | 10.72 | 44.40 | 5.58 |
| M3 | 49.82 | 49.72 | 13.49 | 64.34 | 9.30 |
| M4 | 49.42 | 49.82 | 12.73 | 57.77 | 7.29 |
| M5 | 48.84 | 49.40 | 12.95 | 54.88 | 10.18 |
| M6 | 49.60 | 49.42 | 12.11 | 51.42 | 8.05 |
| M7 | 48.80 | 49.76 | 12.46 | 61.79 | 12.41 |
| M8 | 48.52 | 49.62 | 10.47 | 46.19 | 5.41 |
| M9 | 49.42 | 49.82 | 11.99 | 54.40 | 15.30 |
| M10 | 49.38 | 49.36 | 12.82 | 61.24 | 10.82 |
| M11 | 48.64 | 49.86 | 14.07 | 66.69 | 9.00 |
| M12 | 49.30 | 49.52 | 12.15 | 59.69 | 8.02 |

Stress-strain behavior is considered as one of the most significant characteristics of materials. The dynamic stress-strain curves of coal samples under dynamic loads are shown in Fig. 4. These stress-strain curves go through a gradual descent after the peak stress rather than drop down immediately, which is the most significant difference compared with the stress-strain curves of coal under quasi-static loads. As can be seen from Fig. 4, the dynamic behavior of coal under dynamic loads consists of three evolutionary stages (i.e., stages I, II, III of sample M1). Stage I can be further divided into three parts, namely, OA, AB, and BC. The OA part named compaction stage shows an upward concavity, which is attributed to the closing of pre-existing cracks. Since there are various defects, such as flaws, porous, and joints, in natural coal, the closure of these defects results in a noticeable upward concavity in most stress-strain curves. The compressive capacity of coal gets strengthened after the OA part. The AB part is the linear elastic stage, in which the stress and strain curve increases synchronously and the stress and strain show a positive

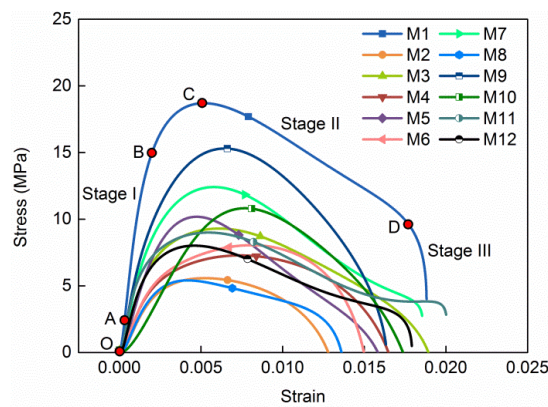


Fig. 4 Dynamic stress-strain curves of coal samples under dynamic loads

linear correlation with steady deformation and elastic energy accumulation in coal body. The BC part is the nonlinear deformation stage, in which the tendency of the stress-strain curve tend to be nonlinearly rising and the slight increase of stress leads to a significant increase in strain. The duration of the BC part is significantly longer than that of the OA and AB parts. At the end of Stage I, the stress-strain curve of coal body shows a peak value (i.e., the dynamic compressive strength), and begins to enter Stage II, which is called the post-peak stage. In Stage II, the coal loses the compressive capacity and the stress decreases gradually while the strain increases rapidly, that is to say, the deformation of coal will continue even if the external loads get removed. Stage III is called the failure stage, in which the stress-strain curve exhibits a rapidly drop down trend, and the coal gets completely decomposed.

3.2 Characteristics of energy dissipation

The dissipated energy and energy dissipation rate of coal specimens under dynamic loads can be calculated using Eqs. (4) and (8), respectively. Fig. 5 shows the relationship between energy dissipation and the strain rate, and Fig. 6 shows the relationship between energy dissipation and incident energy. In these figures, In.Energy represents incident energy, Re.Energy represents reflected energy, Tr.Energy represents transmitted energy, Di.Energy represents dissipated energy, and Di.Energy rate represents energy dissipation rate.

It can be seen from Fig. 5 that with the increase of the strain rate, the incident energy and reflected energy present a synchronous upward trend. Results of correlation analysis showed that the incident energy and the strain rate are subject to a positive linear correlation of $y = 2.93x - 89.51$ (correlation coefficient, 0.94), and that the reflected energy and the strain rate are subject to a positive linear correlation of $y = 2.00x - 54.62$ (correlation coefficient, 0.99). Based on the remarkable positive linear correlation between strain rate and impact velocity (Table 3), and between incident energy and strain rate, we can safely deduce that the higher the impact velocity of striker bar, the more is the incident energy carried by the incident wave.

As can be seen from Fig. 6, the dissipated energy and energy dissipation rate are increased linearly with the incident energy increasing gradually. Results of correlation analysis shows that

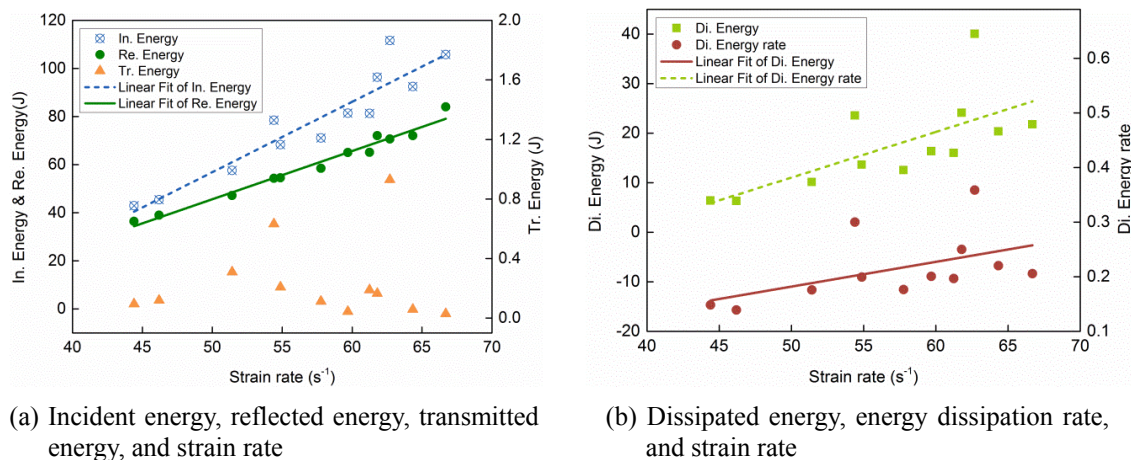


Fig. 5 Relationship between energy dissipation and strain rate

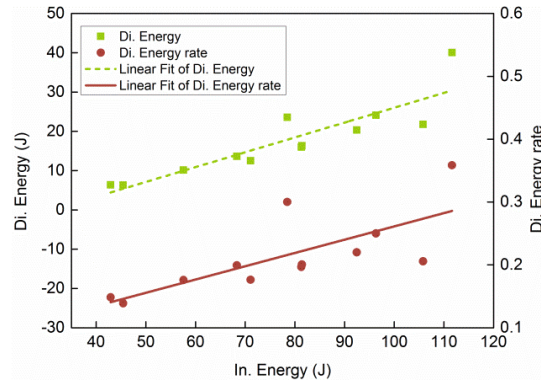
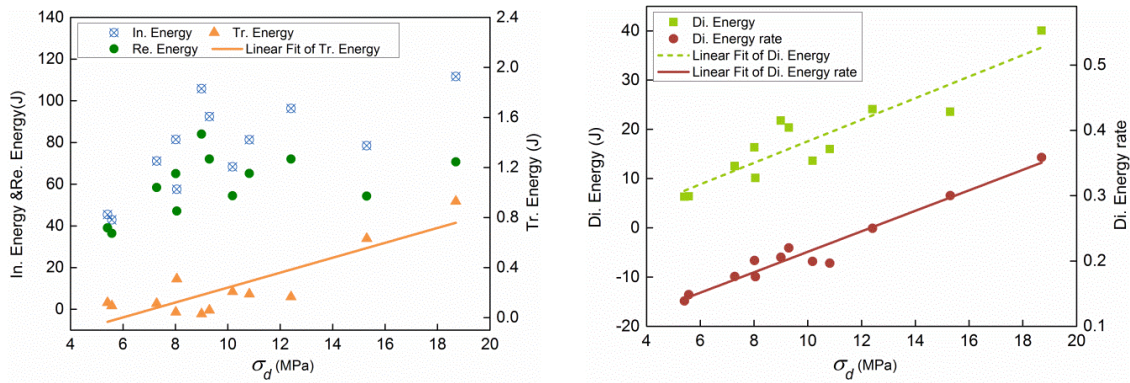


Fig. 6 Relationship between energy dissipation and incident energy



(a) Incident energy, reflected energy, transmitted energy, and dynamic compressive strength

(b) Dissipated energy, energy dissipation rate, and dynamic compressive strength

Fig. 7 Relationship between energy dissipation and dynamic compressive strength (σ_d)

the dissipated energy and energy dissipation rate are positively linearly correlated with the incident energy. The respective correlation functions are $y = 0.38x - 11.76$ and $y = 0.002x + 0.05$, and the corresponding correlation coefficients are 0.89 and 0.74, respectively. Since the incident energy, as well as the strain rate, is positively correlated with the impact velocity of striker bar, it can be concluded that the energy dissipation of coal is closely related to the external loading conditions.

Figs. 7(a) and (b) show the relationship between energy dissipation of coal and its dynamic compressive strength. It can be seen from this Fig. 7(a) that the incident energy, reflected energy, and transmitted energy increased with the increase of the dynamic compressive strength of coal. Results of correlation analysis showed that the dynamic compressive strength is linearly correlated with incident energy and reflected energy, respectively, with corresponding correlation coefficients of 0.69 and 0.46, whereas the correlation coefficient for the relationship between the dynamic compressive strength and transmitted energy is 0.86. This suggests that with improvements in the dynamic compressive strength of coal, the transmitted energy in coal will be increased significantly. Additionally, the dissipated energy and energy dissipation rate are positively linearly correlated with the dynamic compressive strength. The respective correlation functions are $y =$

$2.19x - 4.30$ and $y = 0.016x + 0.057$, and corresponding correlation coefficients are as high as 0.91 and 0.98, suggesting that the higher the dynamic compressive strength of coal under dynamic loading conditions, the more is the dissipated energy of coal.

In order to verify the correlation between incident energy, dynamic compressive strength and the energy dissipation, some existing experimental data of rock (granite, sandstone, limestone, etc.) obtained using SHPB (Hong *et al.* 2009) were analyzed and compared with the results in this study. The results indicate that there is also a good positive relationship between the incident energy, dynamic compressive strength and the energy dissipation, which agrees well with the results in this study. However, the existing literature didn't explain the mechanism of energy dissipation in rock under dynamic loads, thus there is still necessary to give further discussion.

4. Discussion

4.1 Fracture processes of coal under dynamic loads

Since the energy dissipation happens simultaneously with the fracture of coal under dynamic loads, a thorough understanding of the failure mechanism which describes the processes taking place in coal in the course of dynamic loads would be an essential prerequisite for revealing the mechanisms of energy dissipation.

Based on the hypothesis for the mechanism of brittle fracture of rock (Bieniawski 1968), the fracture process in rock from initial load application to complete disintegration of specimen has been divided into following phases: closing of cracks, linear elastic deformation, stable crack propagation, and unstable crack propagation. Since coal is a typical quasi-brittle rock material, the fracture processes of coal under dynamic loads can also be determined from its complete stress-strain curve according to the hypothesis specified above (Fig. 8).

During the first phase called closing of cracks, the pre-existing microscopic pores and cracks in coal gradually closed under the applied dynamic loads, and the compressive capacity has been strengthened through compaction under axial stress. After the completion of crack closure, the stress-strain curves become linear and strain being elastic, which is called the linear elastic deformation phase. It should be noted that the linear elastic deformation phase lasts for a quite

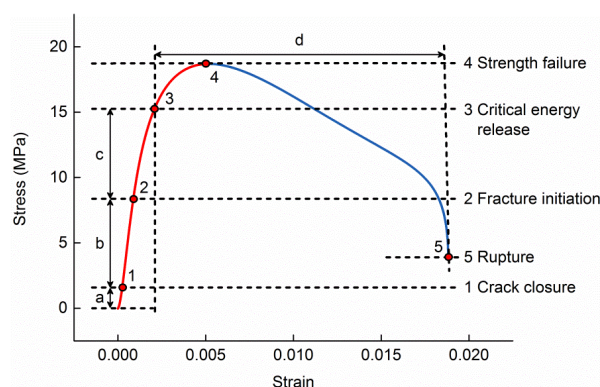


Fig. 8 The fracture processes of coal under dynamic loads. Phase a is closing of cracks, phase b is linear elastic deformation, phase c is stable crack propagation, and phase d is unstable crack propagation

short period under the dynamic loads, and soon further deformation leads to fracture initiation when the closed cracks start to propagate. Now the phase called stable fracture propagation prevails, during this stage, a part of the elastic energy is released to extend the crack surfaces, which is the initiation of energy dissipation. When the applied dynamic loads increase to a certain degree, unstable fracture propagation starts and persist until the final rupture happens. The strength failure occurs during the unstable fracture propagation, which means the coal losses its maximum compressive capacity (i.e., the dynamic strength of coal material). After the strength failure happens, the coal undergoes a rather long period of unstable fracture propagation before the coal rupture occurs, and that, in fact, is the most significant difference compared with that of coal under quasi-static loads. The rupture of coal is the final stage of the fracture processes when the disintegration of coal takes place. The ejected fragments consume the residual elastic energy within coal.

As can be seen from Fig. 8, criteria for stable crack propagation and unstable crack propagation are key points in fracture processes, the criterion for stable crack propagation is also applicable for determining the onset of energy dissipation. Based on the stability concept of brittle fracture, the onset of stable crack propagation is determined by means of the well-known Griffith energy balance at fracture initiation, and the beginning of unstable crack propagation is identified by the Irwin's concept of critical energy release. Since the dynamic loads applied to coal specimen increase rapidly, the fracture initiation and critical energy release occur almost simultaneously, thus resulting in a relatively short stage of stable crack propagation compared with the unstable crack propagation. What's more, after the onset of unstable crack propagation, the crack edge generally accelerates to a very high velocity, which would dissipate a large amount of the elastic energy to sustain crack growth. Hence, in this study, we attribute the most dissipated energy to the unstable crack propagation in fracture processes of coal under dynamic loads.

4.2 Energy dissipation model of coal under dynamic loads

In the SHPB tests on rock materials, assuming that the energy lost at the interfaces between the specimen and the bars is negligible, the dissipated energy, W_c , defined by Eq. (4) is primarily partitioned into three parts: (1) fracture and damage energy, W_G , associated with fracture surface and micro-cracks; (2) kinetic energy, W_K , of flying fragments; (3) other energy, W_O , consumed in other forms of energy such as thermal energy and radiant energy. Since the energy W_O is usually negligible compared with the other forms of energy, the relationship between W_c , W_G , and W_K is generally given as follows (Zhang *et al.* 2000).

$$W_c = W_G + W_K \quad (9)$$

According to a previous experimental study on energy portioning in SHPB tests (Zhang *et al.* 2000), the kinetic energy of flying fragments is a small proportion of the dissipated energy (less than 7%), most of the dissipated energy is used to forming new fracture surfaces and inner cracking damage. Thus, the dissipated energy W_c in Eq. (9) can be approximately rewritten as

$$W_c \approx W_G = G_d A_c \quad (10)$$

where, A_c is the new macro- and micro-fracture surfaces generated in coal under dynamic loads, and G_d is the dynamic energy release rate defined as the rate of mechanical energy flow out the

body and into the crack tip per unit extension (Freund 1998), which equals the dissipated energy per unit extension. The relationship between the dynamic energy release rate and the dynamic stress intensity factor is as follows (Freund 1998).

$$G_d = \frac{1-p^2}{E} [A_I(v)K_{Id}^2 + A_{II}(v)K_{II d}^2] + \frac{1}{2\mu} A_{III}(v)K_{III d}^2 \tag{11}$$

where, E is the modulus of elasticity, μ is the elastic shear modulus, p is the Poisson's ratio, v is the crack speed, K_{Id} , $K_{II d}$, and $K_{III d}$ are dynamic stress intensity factors of three basic modes of crack, $A_I(v)$, $A_{II}(v)$ and $A_{III}(v)$ are universal functions defined as follows (Freund 1998).

$$A_I(v) = \frac{v^2 \alpha_d}{(1-p)c_s^2 [4\alpha_d \alpha_s - (1+\alpha_s^2)^2]} \tag{12}$$

$$A_{II}(v) = \frac{v^2 \alpha_s}{(1-p)c_s^2 [4\alpha_d \alpha_s - (1+\alpha_s^2)^2]} \tag{13}$$

$$A_{III}(v) = 1/\alpha_s \tag{14}$$

where, $\alpha_d = \sqrt{1-(v/C_d)^2}$, $\alpha_s = \sqrt{1-(v/C_s)^2}$, C_d is the dilatational wave speed, C_s is the shear wave speed. The relationship between the dynamic stress intensity factors and static stress intensity factors is summarized as follows (Freund 1998).

$$K_{Id} = k_I(v)K_I, \quad K_{II d} = k_{II}(v)K_{II}, \quad K_{III d} = k_{III}(v)K_{III} \tag{15}$$

where, $k_I(v) \approx (1-v/C_R)/\sqrt{1-v/C_d}$, $k_{II}(v) \approx (1-v/C_R)/\sqrt{1-v/C_s}$, $k_{III}(v) = \sqrt{1-v/C_s}$, C_R is the Rayleigh wave speed, K_I , K_{II} , K_{III} are static stress intensity factors. The expression of static stress intensity factor for different cracks varies from one type to another, but the common form is $K = Y\sigma\sqrt{\pi a}$, where a is the initial crack length, Y is a load-independent constant related to crack geometric parameters only. With the Eqs. (12)-(15) substituted into Eq. (11), we get the dynamic energy release rate given by

$$G_d = \frac{a\pi v^2 \sigma^2 (1-v/C_R)^2 (1+p)}{4EC_s^2 \left(\sqrt{1-\frac{v^2}{C_d^2}} \sqrt{1-\frac{v^2}{C_s^2}} - \left(2-\frac{v^2}{C_s^2}\right)^2 \right)} \left[\frac{Y_I^2 \sqrt{1-v^2/C_d^2}}{1-v/C_d} + \frac{Y_{II}^2 \sqrt{1-v^2/C_s^2}}{1-v/C_s} \right] + \frac{\pi a \sigma^2 Y_{III}^2 \left(1-\frac{v}{C_s}\right)}{2\mu \sqrt{1-\frac{v^2}{C_s^2}}} \tag{16}$$

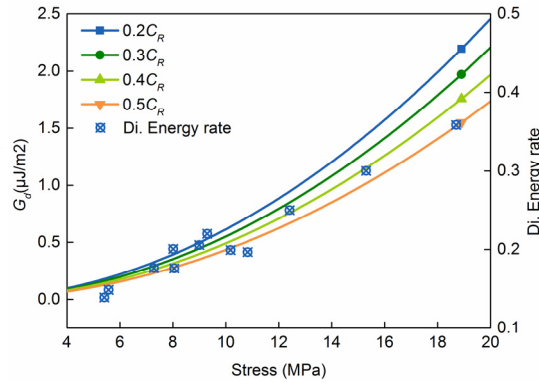


Fig. 9 Theoretical dynamic energy release rate and experimental dissipated energy rate under different stress level. G_d denotes the dynamic energy release rate

It can be concluded from Eq. (16) that the dynamic energy release rate, equivalent to the energy dissipated per unit crack advance, is mainly affected by the crack velocity and the magnitude of loads. According to the aforementioned fracture processes of coal under dynamic loads, the most dissipated energy is caused by unstable crack propagation within coal. Early studies of the unstable fracture propagation process in rock materials have revealed that as the stress level approaches strength failure, the fracture propagates with rapidly increasing velocity, reaching its maximum (i.e., the limiting crack speed) and thereafter constant value at strength failure (Bieniawski 1968). Other experimental studies have shown that the limiting crack speed is a physical constant for nominally brittle materials, and the available maximum crack propagation velocities of rock-like materials under dynamic loads are in the range from $0.2 C_R$ to $0.57 C_R$ (Zhang and Zhao 2014). By substituting the parameters shown in Table 2 into Eq. (16) and the Rayleigh wave speed given by $(0.862 + 1.14p)/(1 + p) C_s$ (Zhang and Zhao 2014), we get the dynamic energy release rate with respect to different crack speed and stress level plotted in Fig. 9.

As a basis for further discussion, we would preannounced that the theoretical dynamic energy release rate shown in Fig. 9 is calculated with assuming that the crack initial length, a , and the crack geometric parameters, Y , is constant. As can be seen from Fig. 9, the dynamic energy release rate, as well as the experimental dissipated energy rate increases synchronously with the increasing stress. Thus a semi-empirical energy dissipation model is proposed based on the expression of dynamic energy release rate (Eq. (16)).

$$w_c = C\sigma^b \quad (17)$$

where, w_c is the energy dissipation rate defined in Eq. (8), C and b are material constants, which are 0.038 and 0.75 for coal specimen in this study. It can be concluded that higher level of stress leads to greater energy released during unstable crack propagation, thus resulting in larger energy dissipation rate of coal under dynamic loads.

5. Conclusions

In this paper, the energy dissipation of coal under dynamic loads is investigated by the experiments conducted using a SHPB system, as well as the theoretical analysis carried out from

the perspective of dynamic fracture processes. The conclusions are as follows:

- The energy dissipation rate are positively linearly correlated with incident energy and dynamic compressive strength, and respective correlation functions are $y = 0.002x + 0.05$ and $y = 0.016x + 0.057$, with correlation coefficients of 0.74 and 0.98.
- The most dissipated energy is attributed to the unstable crack propagation in fracture processes of coal under dynamic loads, higher level of stress leads to greater energy released during unstable crack propagation, thus resulting in larger energy dissipation rate of coal under dynamic loads.
- The positive relationship between dissipated energy rate (w_c) and stress (σ) could be described by an semi-empirical model $w_c = C\sigma^b$, where C and b are material constants, which are 0.038 and 0.75 for coal specimens in this study.

Acknowledgments

The research described in this paper was financially supported by the Research Project of Chinese Ministry of Education (No. 113031A), the National Natural Science Foundation of China (No. 51574231), the Outstanding Innovative Team of China University of Mining and Technology (No. 2014ZY001), and the Priority Academic Program Development of Jiangsu Higher Education Institutions (PAPD).

References

- Aydin, A. (2014), "Upgraded ISRM suggested method for determining sound velocity by ultrasonic pulse transmission technique", *Rock. Mech. Rock. Eng.*, **47**(1), 255-259.
- Bieniawski, Z.T. (1968), "Fracture dynamics of rock", *Int. J. Fract.*, **4**(4), 415-430.
- Bieniawski, Z.T. and Bernede, M.J. (1979), "Suggested methods for determining the uniaxial compressive strength and deformability of rock materials", *Int. J. Rock. Mech. Min.*, **16**(4), 137-140.
- Chen, W.W. and Song, B. (2010), *Split Hopkinson (Kolsky) Bar: Design, Testing and Applications*, Springer, New York, NY, USA.
- Davies, E.D.H. and Hunter, S.C. (1963), "The dynamic compression testing of solids by the method of the split hopkinson pressure bar", *J. Mech. Phys. Solids*, **11**(3), 155-179.
- Freund, L.B. (1998), *Dynamic Fracture Mechanics*, Cambridge University Press, Cambridge, UK.
- Gaziev, E. (2001), "Rupture energy evaluation for brittle materials", *Int. J. Solids. Struct.*, **38**(42-43), 7681-7690.
- Hong, L., Zhou, Z.L., Yin, T.B., Liao, G.Y. and Ye, Z.Y. (2009), "Energy consumption in rock fragmentation at intermediate strain rate", *J. Cent. South Univ. Technol.*, **16**(4), 677-682.
- Huang, D. and Li, Y.R. (2014), "Conversion of strain energy in triaxial unloading tests on marble", *Int. J. Rock. Mech. Min.*, **66**(2), 160-168.
- Li, M., Mao, X., Lu, A., Tao, J., Zhang, G., Zhang, L. and Li, C. (2014), "Effect of specimen size on energy dissipation characteristics of red sandstone under high strain rate", *Int. J. Min. Sci. Technol.*, **24**(2), 151-156.
- Liu, J.Z., Xu, J.Y., Lv, X.C., Zhao, D.H. and Leng, B.L. (2012), "Experimental study on dynamic mechanical properties of amphibolites, sericite-quartz schist and sandstone under impact loadings", *Int. J. Nonlinear Sci. Numer. Simul.*, **13**(2), 209-217.
- Lundberg, B. (1976), "A split Hopkinson bar study of energy absorption in dynamic rock fragmentation", *Int. J. Rock. Mech. Min.*, **13**(6), 187-197.

- Peng, R.D., Ju, Y., Wang, J.G., Xie, H.P., Gao, F. and Mao, L.T. (2015), "Energy dissipation and release during coal failure under conventional triaxial compression", *Rock. Mech. Rock. Eng.*, **48**(2), 509-526.
- Song, D.Z., Wang, E.Y. and Liu, J. (2012), "Relationship between EMR and dissipated energy of coal rock mass during cyclic loading process", *Safety Sci.*, **50**(4), 751-760.
- Song, D., Wang, E., Li, Z., Liu, J. and Xu, W. (2015), "Energy dissipation of coal and rock during damage and failure process based on EMR", *Int. J Min. Sci. Technol.*, **25**(5), 787-795.
- Sufian, A. and Russell, A.R. (2013), "Microstructural pore changes and energy dissipation in Gosford sandstone during pre-failure loading using X-ray CT", *Int. J. Rock. Mech. Min.*, **57**(1), 119-131.
- Wasantha, P.L.P., Ranjith, P.G. and Shao, S.S. (2014), "Energy monitoring and analysis during deformation of bedded-sandstone: Use of acoustic emission", *Ultrasonics*, **54**(1), 217-226.
- Whittles, D.N., Kingman, S., Lowndes, I. and Jackson, K. (2006), "Laboratory and numerical investigation into the characteristics of rock fragmentation", *Miner. Eng.*, **19**(14), 1418-1429.
- Xie, H.P., Li, L.Y., Ju, Y., Peng, R.D. and Yang, Y.M. (2011), "Energy analysis for damage and catastrophic failure of rocks", *Sci. China-Technol. Sci.*, **54**(Suppl. 1), 199-209.
- Yang, L., Yang, R., Qu, G. and Zhang, Y. (2014), "Caustic study on blast-induced wing crack behaviors in dynamic-static superimposed stress field", *Int. J Min. Sci. Technol.*, **24**(4), 417-423.
- Zhang, Q.B. and Zhao, J. (2014), "A review of dynamic experimental techniques and mechanical behaviour of rock materials", *Rock. Mech. Rock. Eng.*, **47**(4), 1411-1478.
- Zhang, Z.X., Kou, S.Q., Jiang, L.G. and Lindqvist, P.A. (2000), "Effects of loading rate on rock fracture: fracture characteristics and energy partitioning", *Int. J. Rock. Mech. Min.*, **37**(7), 745-762.
- Zhou, Y.X., Xia, K., Li, X.B., Li, H.B., Ma, G.W., Zhao, J., Zhou, Z.L. and Dai, F. (2012), "Suggested methods for determining the dynamic strength parameters and mode-I fracture toughness of rock materials", *Int. J. Rock. Mech. Min.*, **49**(1), 105-112.